https://doi.org/10.5194/mr-2024-21
Preprint. Discussion started: 19 November 2024

MAGNETIC RESONANCE
Open Access
Discussions

Pseudo Rotary Resonance Relaxation Dispersion Effects in Isotropic Samples

Authors: *Evgeny Nimerovsky*, Jonas Mehrens & Loren B. Andreas**

Affiliations:

Department of NMR based Structural Biology, Max Planck Institute for Multidisciplinary Sciences, Am Faßberg 11, Göttingen, Germany

*Corresponding authors: land@mpinat.mpg.de ORCID: 0000-0003-3216-9065 and evni@mpinat.mpg.de ORCID: 0000-0003-3002-0718.

Abstract

Enhanced transverse relaxation near rotary-resonance conditions is a well-documented effect for anisotropic solid samples undergoing magic-angle spinning (MAS). It is a surprising behavior for rotating liquids, in which first-order anisotropic interactions are averaged at a much faster timescale as compared with the spinning frequency. Here we report measurements of ^{13}C transverse relaxation under spin lock for spinning samples of both polybutadiene rubber and polyethylene glycol solution. Maxima in the relaxation rates are observed when the spin-lock frequency matches one or two times the MAS rate. Through simulations, we qualitatively describe the appearance of this effect, which can be explained by time dependence caused by sample rotation and an inhomogeneous rf-field distribution. Consideration of this effect is important for MAS experiments based on rotary-resonance conditions, and motivates the design of new MAS coils with improved rf-field homogeneity.

https://doi.org/10.5194/mr-2024-21
Preprint. Discussion started: 19 November 2024

MAGNETIC RESONANCE
Open Access
Discussions

KEYWORDS: Magic-angle spinning, nuclear magnetic resonance spectroscopy, pseudo rotary-resonance relaxation-dispersion effect

Introduction

Measurement of the transverse relaxation rates of nuclear spins as a function of the applied rf-field spin-lock strengths is an elegant and well-established method for detecting structural molecular dynamics.(Abyzov et al., 2022; Alam et al., 2024; Camacho-Zarco et al., 2022; Hu et al., 2021; Massi and Peng, 2018; Palmer, 2015; Palmer and Massi, 2006; Pratihar et al., 2016; Rangadurai et al., 2019; Sekhar and Kay, 2019; Stief et al., 2024) For molecular solids, rocking motion or slow exchange in organic and inorganic samples(Fonseca et al., 2022; Keeler and McDermott, 2022; Krushelnitsky et al., 2018, 2023; Kurauskas et al., 2017; Lewandowski et al., 2011; Ma et al., 2014; Marion et al., 2019; Öster et al., 2019; Quinn and McDermott, 2009; Rovó and Linser, 2018; Shcherbakov et al., 2023; Vugmeyster et al., 2023) under MAS(Andrew et al., 1958; Lowe, 1959) NMR have been studied via the impact on transverse relaxation. This detection can be achieved by performing a spin-lock experiment,(Furman et al., 1998) where the decay of magnetization is measured as a function of the power of the applied SL-pulse (spin-lock pulse). For slow motion or slow exchange in the microsecond (μs) range, the spectral densities(Redfield, 1957) of the investigated spins may include additional terms(Kurbanov et al., 2011; Marion et al., 2019) that arise from non-averaged anisotropic interactions.(Kurbanov et al., 2011; Rovó, 2020; Schanda and Ernst, 2016) These terms depend on the sums and differences between the nutation frequency induced by the rf-field (ν_{SL}=γB_1/(2π)) and MAS rate (ν_R). Such dependence causes a significant increase in the measured relaxation rates when ν_{SL} approaches one of the rotary-resonance conditions ($\nu_{SL} = \nu_R$ or $2\nu_R$).(Marion et al., 2019)

https://doi.org/10.5194/mr-2024-21
Preprint. Discussion started: 19 November 2024

For liquid samples, where SL experiments are routinely used to detect fast exchange,(Cavanagh et al., 2006; Deverell et al., 1970; Palmer, 2004) sample rotation is not expected to induce any rotary-resonance conditions based on anisotropic spin interactions,(Levitt et al., 1988; Oas et al., 1988) since such interactions are eliminated by nanosecond-timescale isotropic motion.(Haeberlen and Waugh, 1968; Maricq, 1982) However, to our surprise, we still observed changes in the relaxation rate at rotary-resonance conditions for liquid and liquid-like samples during SL experiments. In this article, we demonstrate these observations using natural abundance ^{13}C polybutadiene rubber at 10 kHz, 20 kHz and 35 kHz MAS. The same behavior is observed for a polyethylene glycol solution at 10 kHz MAS. We chose these samples since the polybutadiene rubber displays liquid-like spectra but does not undergo translational diffusion due to the elastomeric properties of a cross-linked polymer. On the other hand, since the polybutadiene is an elastomer and therefore may not undergo perfect isotropic averaging, we also recorded data for a polyethylene glycol solution that is sure to undergo nanosecond isotropic averaging. Through numerical simulations,(Nimerovsky and Goldbourt, 2012) we show that this behavior can be qualitatively explained by the influence of the periodic component of the applied rf-field, which arises from the rotation of the sample in a spatially inhomogeneous rf-field.(Tošner et al., 2017)

Results and Discussion

Figure 1 displays the spin-lock sequence. Similar to previously proposed versions,(Vugmeyster et al., 2022) it contains a heat compensation block (HC), followed by a π/2-pulse, T_2 −filter(Schmidt-Rohr et al., 1992) (to reduce any broad signal components from the polymer) and a spin-lock pulse (SL). The mixing times for HC and SL pulses were the same during a single experiment ($t_{HC} = t_{SL} = N_{SL}T_R$), while the sum of the rf-field powers of these

https://doi.org/10.5194/mr-2024-21
Preprint. Discussion started: 19 November 2024

applied pulses always equaled to a fixed value. In all experiments, we used continuous HC and SL (Figure 1B) except in one (the data is shown in Figure 2C), where we applied windowed pulses (Figure 1B). During acquisition, WALTZ16 decoupling(Shaka et al., 1983) was used.

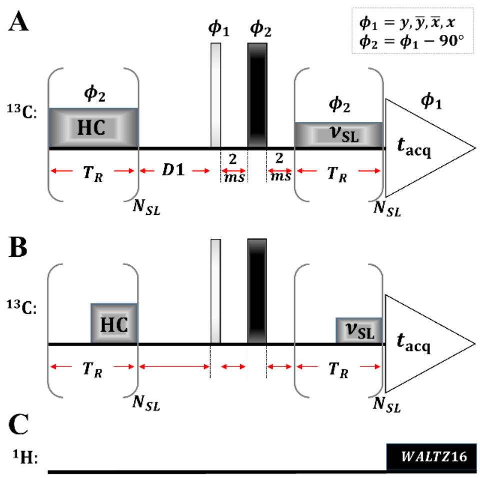

Figure 1 Spin-lock sequence with heat compensation (HC), T_2 −filter (2 ms – π-pulse – 2ms) and spin-lock (SL) blocks. The SL and HC elements consisted of a train of N_{SL} rotor-synchronized continuous (A) or windowed (B) pulses with the same phase (ϕ_2) and rf-field strength (ν_{SL}). In all experiments, $power_{HC} + power_{SL}$ =constant (equivalent to 50 kHz rf-field strength). During acquisition, WALTZ-16 decoupling(Shaka et al., 1983) (C) was applied on the ^{1}H channel.

The experimental SL profiles under three different MAS rates: 10 kHz (A and C), 20 kHz (D) and 35 kHz (B) are shown in Figure 2. For Figures 2A, 2B and 2D, a drastic change in the relaxation rate is observed at rotary-resonance conditions when ν_{SL} equals either ν_R or $2\nu_R$. For Figure 2C, we used 10 kHz MAS and windowed pulses: half of the rotor period is a window, as shown in Figure 1B. Under these conditions, a drastic change in the relaxation rate is observed when ν_{SL} equals either to $2\nu_R$ or $4\nu_R$. We previously observed similar behavior for windowed CP profiles,(Nimerovsky et al., 2023) where increasing the window between rotor-synchronized

https://doi.org/10.5194/mr-2024-21
Preprint. Discussion started: 19 November 2024

pulses from zero to half a rotor period doubled the required rf-field strength for cross-polarization transfers.(Hartmann and Hahn, 1962) Interestingly, with windowed pulses, the SL profile appears similar to that with continuous pulses, and even under a low rf-field strength of 1 kHz, there is no change in the $T_{1\rho}$ relaxation time (Figure S2A in SI). The experimental spin-echo(Hahn, 1950) and inversion recovery(Vold et al., 1968) curves for this sample are illustrated in Figure S2.

From Figure 2, we can also observe that the location of the first minimum signal intensity in the experimental SL profiles depends on the MAS rate (indicated in gray in Figure 2). For 10 kHz MAS (Figure 2A and 2C), the locations are approximately at a 3 ms SL time, while for 20 kHz (Figure 2D) and 35 kHz (Figure 2B), the locations are approximately at 1 ms and 0.4 ms, respectively. However, in all four profiles at these minimum points, the signal reaches a similar value of approximately 0.53.

Rotary-resonance conditions at ν_R and $2\nu_R$ of rf-field strength are also observed for the polyethylene glycol sample at 10 kHz MAS (Figure S3 in SI). The performance of the SL experiments on both samples helps rule out the influence of translational diffusion(Hahn, 1950) (which may be present for polyethylene glycol but not for polybutadiene rubber) or residual dipolar interaction(Cohen-Addad and Vogin, 1974) (which might be present for polybutadiene rubber but is not relevant for polyethylene glycol).

https://doi.org/10.5194/mr-2024-21
Preprint. Discussion started: 19 November 2024

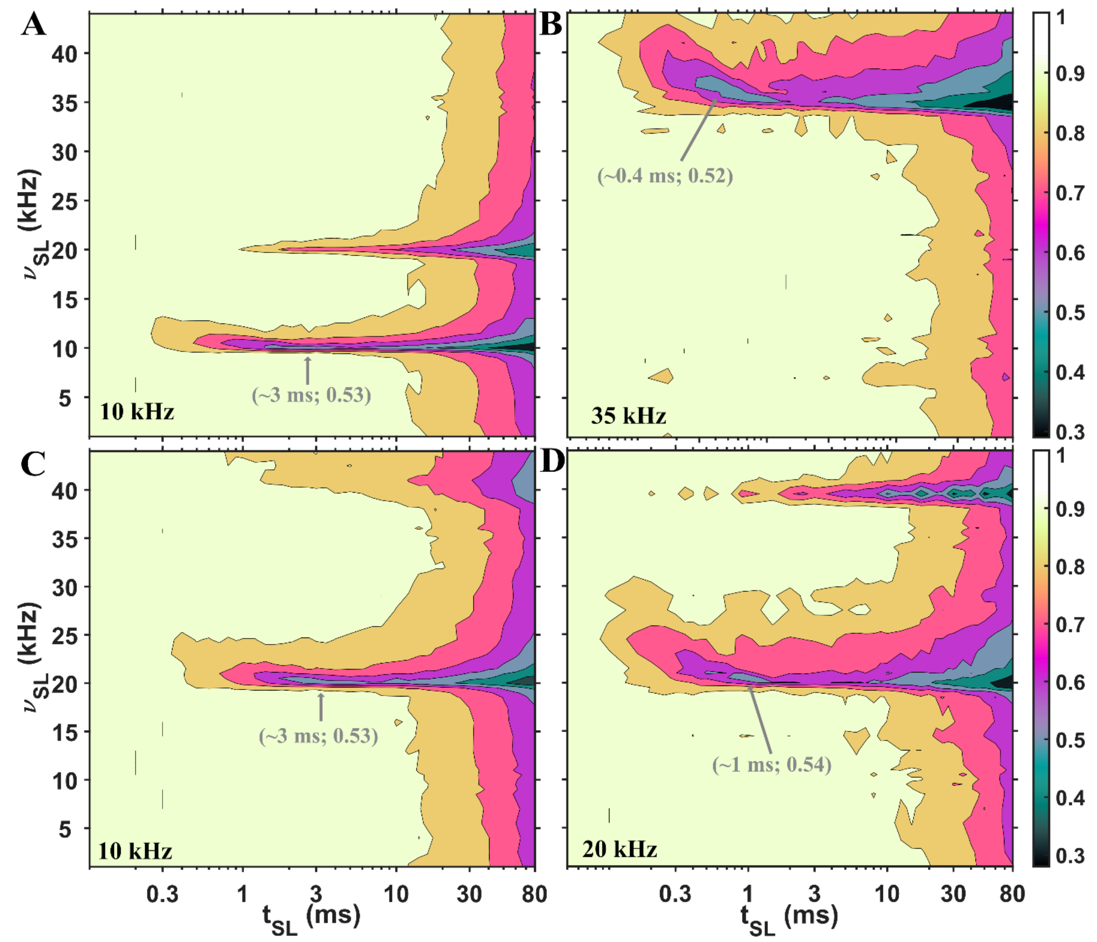

Figure 2 ^{13}C polybutadiene rubber signal is shown as functions of the rf-field strength (ν_{SL}, y-axis) and mixing time (t_{SL}, x-axis) of the SL under three different MAS rates: 10 kHz (A and C), 20 kHz (D) and 35 kHz (B). For (A), (B) and (D), continuous SL was applied, while for (C), windowed (half rotor period was filled with the pulse) SL was implemented. The values in gray represent the coordinates of the first minimum in the profiles. Additional experimental details are provided in the supplementary information (SI).

To understand the major source of the apparent rotary-resonance conditions in liquid and liquid-like samples, we performed numerical simulations. In these simulations, two scenarios were considered in which the external magnetic fields (B_0 or B_1) gained time dependence due to the rotation of the sample and:

https://doi.org/10.5194/mr-2024-21
Preprint. Discussion started: 19 November 2024

Open Access MAGNETIC RESONANCE Discussions

- A spatially inhomogeneous external magnetic field strength (Figure 3, Figure S1A and Eqn. S3A in SI),
- A spatially inhomogeneous rf-field strength (Figure 4, Figure S1B and Eqn. S3B in SI).

Note that the first scenario is compatible with a narrow linewidth under MAS.(Sodickson and Cory, 1997)

For each scenario, a time independent distribution of rf-field strength was also included (Figure S1C and Eqn. S3C in SI). Its profile and influence has been investigated previously(Engelke, 2002; Gupta et al., 2015; Hoult, 1976; Paulson et al., 2004; Tošner et al., 2017, 2018) and in our experiments it was found to broaden rotary-resonance conditions. This type of inhomogeneity is expected for solenoidal coils in which the sample near the ends of the coil experiences a lower rf-field strength. For simplicity, we did not include a time-independent distribution of external magnetic field strength,(Hoult, 1976; Hürlimann and Griffin, 2000) as it had a minor effect in our experiments, and shimming under MAS ensures that it is minimal.

Figure 3 shows simulations for the first scenario. While some similarities between Figure 2 and Figure 3 are observed, there are three major differences in the SL profiles, which should be highlighted. Firstly, in Figure 3, the intensities at the first minima show a dependence on MAS rate (marked in gray in Figure 3), whereas in Figure 2, the experimental profiles show only a slight dependence. Secondly, in Figure 3, the locations of these minima in time (x-axis) do not depend on the MAS rate (Figure 3A, 3B and 3D), whereas the location in time changes when windowed pulses are applied (Figure 3C). In contrast, the experimental profiles exhibit the reverse behavior. Thirdly, in Figure 3C, only a single rotary-resonance condition is observed, while in Figure 2C, two rotary-resonance conditions are detected. Additionally, increasing the

https://doi.org/10.5194/mr-2024-21
Preprint. Discussion started: 19 November 2024

MAGNETIC RESONANCE
Open Access
Discussions

magnetic field inhomogeneity by deliberately mis-setting the room temperature shims had little influence on the SL profile (shown in Figure S4 in the SI).

All of this indicates that a spatially inhomogeneous external magnetic field cannot be a major source of the appearance of rotary-resonances conditions in rotating liquids and liquid-like samples.

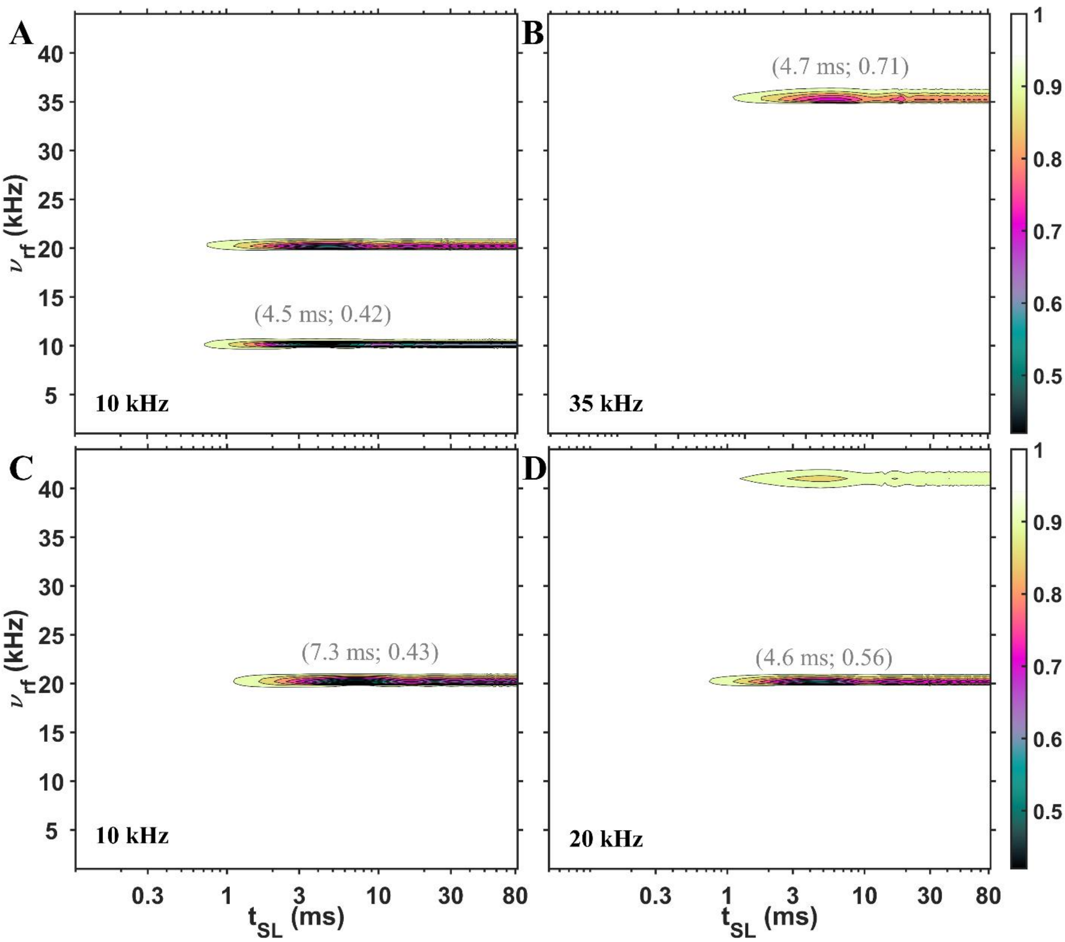

Figure 3 Simulated SL profiles showing the influence of time dependence introduced via an inhomogeneous external magnetic field. The simulated signal is shown as a function of the rf-field strength (ν_{SL}, axis y) and mixing time (t_{SL}, axis x) of the SL under three different MAS rates: 10 kHz (A and C), 20 kHz (D) and 35 kHz (B). For (A),

https://doi.org/10.5194/mr-2024-21
Preprint. Discussion started: 19 November 2024

MAGNETIC RESONANCE
Open Access
Discussions

(B) and (D), continuous SL was applied, while for (C) windowed SL was implemented (half rotor period was filled with the pulse). The values in gray represent the coordinates of the first minima in the profiles. No phenomenological relaxation was included in the simulations. Additional simulated details are provided in the SI.

In contrast, simulations of SL profiles with time dependence introduced via a spatially inhomogeneous rf-field (Figure 4) qualitatively agree with the experimental plots, indicating that a spatially inhomogeneous rf-field is a better explanation for the appearance of rotary-resonance conditions in rotating liquids and liquid-like samples using conventional MAS NMR probes with solenoidal coils. Such time dependence has been previously considered in the design of magnetization transfer elements using optimal control.(Blahut et al., 2022, 2023; Glaser et al., 2015; Joseph and Griesinger, 2023; Tošner et al., 2017, 2018)

This qualitative explanation, provided by simulations, indicates that this effect can also be anticipated in experiments involving solid samples, in addition to the desired effects caused by molecular motion. It is therefore recommended to consider coil inhomogeneity when measuring relaxation rates near rotary resonance conditions. Fortunately, the magnitude of this effect is considerably smaller than the strong relaxation observed in recent reports that detected slow structural dynamics via near rotary resonance conditions.(Krushelnitsky et al., 2018)

https://doi.org/10.5194/mr-2024-21
Preprint. Discussion started: 19 November 2024

MAGNETIC RESONANCE
Open Access
Discussions

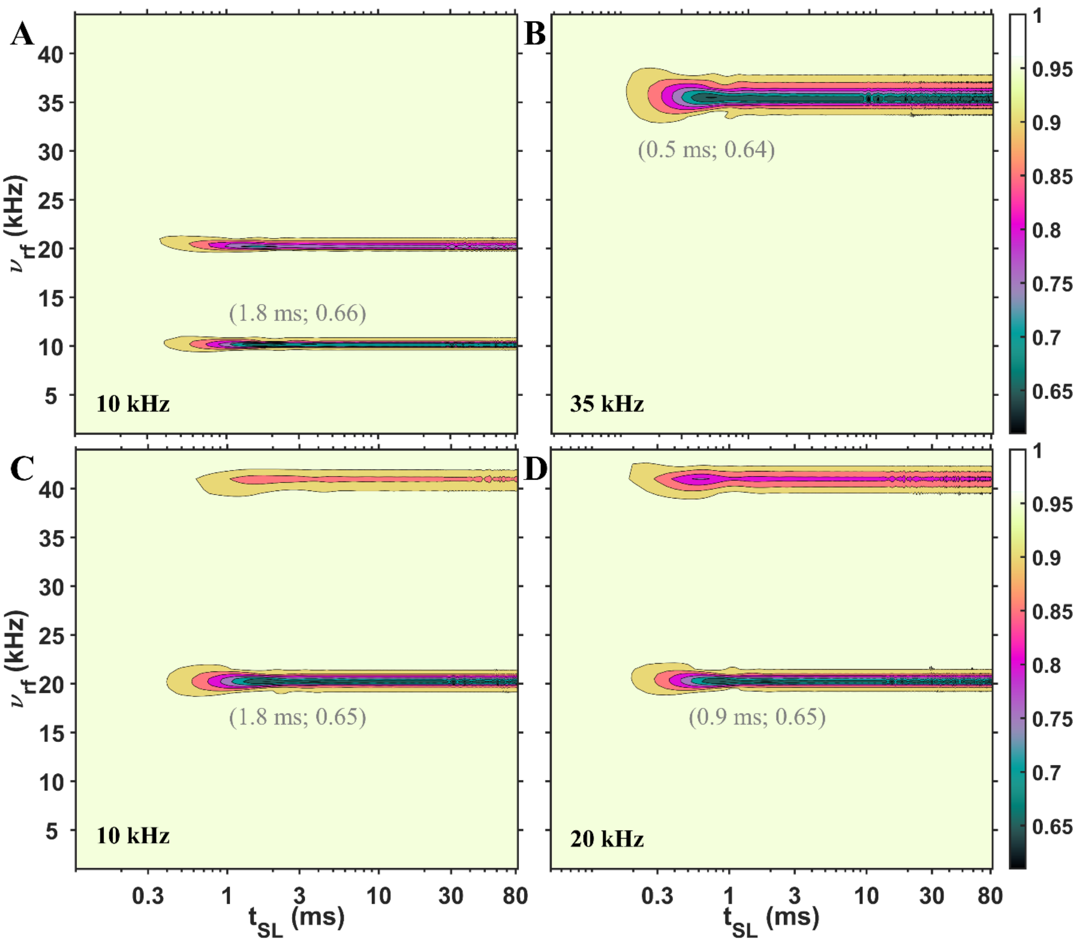

Figure 4 The influence of the inhomogeneous rf-field on the simulated SL profiles. The simulated signal is shown as functions of the rf-field strength (ν_{SL}, axis y) and mixing time (t_{SL}, axis x) of the SL under three different MAS rates: 10 kHz (A and C), 20 kHz (D) and 35 kHz (B). For (A), (B) and (D), continuous SL was applied, while for (C) windowed (half rotor period was filled with the pulse) SL was implemented. The values in gray represent the coordinates of the first minima points in the profiles. Relaxation rates were not included into the simulations. Additional simulated details are provided in the SI.

Conclusions

Rotary-resonance conditions, under which the applied rf-field strength equals an even multiple of the MAS rate, provide a powerful avenue to obtain specific structural information via recoupling of anisotropic interactions in solids(De Paëpe, 2012; Nishiyama et al., 2022) or for detecting changes in the relaxation rates due to slow motion in the μs range.(Rovó, 2020) Canonically, rotary-resonance conditions are not expected in liquids due to the averaging of first-order anisotropic interactions from (sub) nanosecond isotropic motion.(Haeberlen and Waugh, 1968; Maricq, 1982) In this article, we presented experimental data, in which we detected rotary-resonance conditions in a liquid and a liquid-like sample. We qualitatively explained the major source of these conditions, which can occur from a combination of two factors: the rotation of the sample and a spatially inhomogeneous rf-field produced a solenoidal coil.(Tošner et al., 2017) As a result, the rf-field Hamiltonian contains time-dependent terms, which leads to signal loss, i.e. pseudo relaxation behavior, at or near rotary-resonance conditions. To mitigate these effects, it may be advantageous to consider different hardware designs,(Chen et al., 2018; Xu et al., 2021) for example rf coils that produce more homogeneous rf-fields.(Grant et al., 2010; Kelz et al., 2019; Krahn et al., 2008; Stringer et al., 2005)

Competing interests

The contact author has declared that none of the authors has any competing interests.

Acknowledgments

We acknowledge financial support from the MPI for Multidisciplinary Sciences, and from the Deutsche Forschungsgemeinschaft (Emmy Noether program Grant AN1316/1-2). We thank Dr. Supriya Pratihar for inspiring this work by noticing enhanced relaxation at rotor resonance conditions in exploratory high-power relaxation dispersion measurements in a 0.7 mm MAS probe. We thank Dr. Dirk Bockelmann and Brigitta Angerstein for technical assistance.

Author contribution

EN and LBA designed the experiments. EN and JM recorded NMR data and ran simulations, EN and LBA wrote the article. All authors edited and approved the article.

References

Abyzov, A., Blackledge, M., and Zweckstetter, M.: Conformational Dynamics of Intrinsically Disordered Proteins Regulate Biomolecular Condensate Chemistry, Chem. Rev., 122, 6719–6748, https://doi.org/10.1021/acs.chemrev.1c00774, 2022.

Alam, M. K., Bhuvaneshwari, R. A., and Sengupta, I.: 19F NMR relaxation of buried tryptophan side chains suggest anisotropic rotational diffusion of the protein RfaH, J. Biomol. NMR, https://doi.org/10.1007/s10858-024-00450-x, 2024.

Andrew, E. R., Bradbury, A., and Eades, R. G.: Nuclear Magnetic Resonance Spectra from a Crystal rotated at High Speed, Nature, 182, 1659–1659, https://doi.org/10.1038/1821659a0, 1958.

Blahut, J., Brandl, M. J., Pradhan, T., Reif, B., and Tošner, Z.: Sensitivity-Enhanced Multidimensional Solid-State NMR Spectroscopy by Optimal-Control-Based Transverse Mixing Sequences, J. Am. Chem. Soc., https://doi.org/10.1021/jacs.2c06568, 2022.

Blahut, J., Brandl, M. J., Sarkar, R., Reif, B., and Tošner, Z.: Optimal control derived sensitivity-enhanced CA-CO mixing sequences for MAS solid-state NMR – Applications in sequential protein backbone assignments, J. Magn. Reson. Open, 16–17, 100122, https://doi.org/10.1016/j.jmro.2023.100122, 2023.

Camacho-Zarco, A. R., Schnapka, V., Guseva, S., Abyzov, A., Adamski, W., Milles, S., Jensen, M. R., Zidek, L., Salvi, N., and Blackledge, M.: NMR Provides Unique Insight into the Functional Dynamics and Interactions of Intrinsically Disordered Proteins, Chem. Rev., 122, 9331–9356, https://doi.org/10.1021/acs.chemrev.1c01023, 2022.

Cavanagh, J., Fairbrother, W. J., Palmer, A. G., III., Rance, M., and Skelton, N. J.: Protein NMR Spectroscopy: Principles and Practice, 1 pp., 2006.

Chen, P., Albert, B. J., Gao, C., Alaniva, N., Price, L. E., Scott, F. J., Saliba, E. P., Sesti, E. L., Judge, P. T., Fisher, E. W., and Barnes, A. B.: Magic angle spinning spheres, Sci. Adv., 4, eaau1540, https://doi.org/10.1126/sciadv.aau1540, 2018.

Cohen-Addad, J. P. and Vogin, R.: Molecular Motion Anisotropy as Reflected by a “Pseudosolid” Nuclear Spin Echo: Observation of Chain Constraints in Molten cis-1, 4-Polybutadiene, Phys. Rev. Lett., 33, 940–943, https://doi.org/10.1103/PhysRevLett.33.940, 1974.

De Paëpe, G.: Dipolar Recoupling in Magic Angle Spinning Solid-State Nuclear Magnetic Resonance, Annu. Rev. Phys. Chem., 63, 661–684, https://doi.org/10.1146/annurev-physchem-032511-143726, 2012.

Deverell, C., Morgan, R. E., and Strange, J. H.: Studies of chemical exchange by nuclear magnetic relaxation in the rotating frame, Mol. Phys., 18, 553–559, https://doi.org/10.1080/00268977000100611, 1970.

Engelke, F.: Electromagnetic wave compression and radio frequency homogeneity in NMR solenoidal coils: Computational approach, Concepts Magn. Reson., 15, 129–155, https://doi.org/10.1002/cmr.10029, 2002.

Fonseca, R., Vieira, R., Sardo, M., Marin-Montesinos, I., and Mafra, L.: Exploring Molecular Dynamics of Adsorbed CO2 Species in Amine-Modified Porous Silica by Solid-State NMR Relaxation, J. Phys. Chem. C, 126, 12582–12591, https://doi.org/10.1021/acs.jpcc.2c02656, 2022.

Furman, G. B., Panich, A. M., and Goren, S. D.: Spin-locking in one pulse NMR experiment, Solid State Nucl. Magn. Reson., 11, 225–230, https://doi.org/10.1016/S0926-2040(97)00108-2, 1998.

Glaser, S. J., Boscain, U., Calarco, T., Koch, C. P., Köckenberger, W., Kosloff, R., Kuprov, I., Luy, B., Schirmer, S., Schulte-Herbrüggen, T., Sugny, D., and Wilhelm, F. K.: Training Schrödinger's cat: quantum optimal control, Eur. Phys. J. D, 69, 279, https://doi.org/10.1140/epjd/e2015-60464-1, 2015.

Grant, C. V., Wu, C. H., and Opella, S. J.: Probes for high field solid-state NMR of lossy biological samples, J. Magn. Reson., 204, 180–188, https://doi.org/10.1016/j.jmr.2010.03.011, 2010.

Gupta, R., Hou, G., Polenova, T., and Vega, A. J.: RF Inhomogeneity and how it Control CPMAS, Solid State Nucl. Magn. Reson., 72, 17–26, https://doi.org/10.1016/j.ssnmr.2015.09.005, 2015.

Haeberlen, U. and Waugh, J. S.: Coherent Averaging Effects in Magnetic Resonance, Phys. Rev., 175, 453–467, https://doi.org/10.1103/PhysRev.175.453, 1968.

Hahn, E. L.: Spin Echoes, Phys. Rev., 80, 580–594, https://doi.org/10.1103/PhysRev.80.580, 1950.

Hartmann, S. R. and Hahn, E. L.: Nuclear Double Resonance in the Rotating Frame, Phys. Rev., 128, 2042–2053, https://doi.org/10.1103/PhysRev.128.2042, 1962.

Hoult, D. I.: Solvent peak saturation with single phase and quadrature fourier transformation, J. Magn. Reson. 1969, 21, 337–347, https://doi.org/10.1016/0022-2364(76)90081-0, 1976.

Hu, Y., Cheng, K., He, L., Zhang, X., Jiang, B., Jiang, L., Li, C., Wang, G., Yang, Y., and Liu, M.: NMR-Based Methods for Protein Analysis, Anal. Chem., 93, 1866–1879, https://doi.org/10.1021/acs.analchem.0c03830, 2021.

Hürlimann, M. D. and Griffin, D. D.: Spin Dynamics of Carr–Purcell–Meiboom–Gill-like Sequences in Grossly Inhomogeneous *B*0 and *B*1 Fields and Application to NMR Well Logging, J. Magn. Reson., 143, 120–135, https://doi.org/10.1006/jmre.1999.1967, 2000.

Joseph, D. and Griesinger, C.: Optimal control pulses for the 1.2-GHz (28.2-T) NMR spectrometers, Sci. Adv., 9, eadj1133, https://doi.org/10.1126/sciadv.adj1133, 2023.

Keeler, E. G. and McDermott, A. E.: Rotating Frame Relaxation in Magic Angle Spinning Solid State NMR, a Promising Tool for Characterizing Biopolymer Motion, Chem. Rev., 122, 14940–14953, https://doi.org/10.1021/acs.chemrev.2c00442, 2022.

Kelz, J. I., Kelly, J. E., and Martin, R. W.: 3D-printed dissolvable inserts for efficient and customizable fabrication of NMR transceiver coils, J. Magn. Reson., 305, 89–92, https://doi.org/10.1016/j.jmr.2019.06.008, 2019.

Krahn, A., Priller, U., Emsley, L., and Engelke, F.: Resonator with reduced sample heating and increased homogeneity for solid-state NMR, J. Magn. Reson., 191, 78–92, https://doi.org/10.1016/j.jmr.2007.12.004, 2008.

Krushelnitsky, A., Gauto, D., Rodriguez Camargo, D. C., Schanda, P., and Saalwächter, K.: Microsecond motions probed by near-rotary-resonance R1ρ 15N MAS NMR experiments: the model case of protein overall-rocking in crystals, J. Biomol. NMR, 71, 53–67, https://doi.org/10.1007/s10858-018-0191-4, 2018.

Krushelnitsky, A., Hempel, G., Jurack, H., and Mendes Ferreira, T.: Rocking motion in solid proteins studied by the 15 N proton-decoupled R 1ρ relaxometry, Phys. Chem. Chem. Phys., 25, 15885–15896, https://doi.org/10.1039/D3CP00444A, 2023.

Kurauskas, V., Izmailov, S. A., Rogacheva, O. N., Hessel, A., Ayala, I., Woodhouse, J., Shilova, A., Xue, Y., Yuwen, T., Coquelle, N., Colletier, J.-P., Skrynnikov, N. R., and Schanda, P.: Slow conformational exchange and overall rocking motion in ubiquitin protein crystals, Nat. Commun., 8, 145, https://doi.org/10.1038/s41467-017-00165-8, 2017.

Kurbanov, R., Zinkevich, T., and Krushelnitsky, A.: The nuclear magnetic resonance relaxation data analysis in solids: General *R* 1/ *R* 1 *ρ* equations and the model-free approach, J. Chem. Phys., 135, 184104, https://doi.org/10.1063/1.3658383, 2011.

Levitt, M. H., Oas, T. G., and Griffin, R. G.: Rotary Resonance Recoupling in Heteronuclear Spin Pair Systems, Isr. J. Chem., 28, 271–282, https://doi.org/10.1002/ijch.198800039, 1988.

Lewandowski, J. R., Sass, H. J., Grzesiek, S., Blackledge, M., and Emsley, L.: Site-Specific Measurement of Slow Motions in Proteins, J. Am. Chem. Soc., 133, 16762–16765, https://doi.org/10.1021/ja206815h, 2011.

Lowe, I. J.: Free Induction Decays of Rotating Solids, Phys. Rev. Lett., 2, 285–287, https://doi.org/10.1103/PhysRevLett.2.285, 1959.

Ma, P., Haller, J. D., Zajakala, J., Macek, P., Sivertsen, A. C., Willbold, D., Boisbouvier, J., and Schanda, P.: Probing Transient Conformational States of Proteins by Solid-State R1ρ Relaxation-Dispersion NMR Spectroscopy, Angew. Chem. Int. Ed., 53, 4312–4317, https://doi.org/10.1002/anie.201311275, 2014.

Maricq, M. M.: Application of average Hamiltonian theory to the NMR of solids, Phys. Rev. B, 25, 6622–6632, https://doi.org/10.1103/PhysRevB.25.6622, 1982.

Marion, D., Gauto, D. F., Ayala, I., Giandoreggio-Barranco, K., and Schanda, P.: Microsecond Protein Dynamics from Combined Bloch-McConnell and Near-Rotary-Resonance R1 Relaxation-Dispersion MAS NMR, ChemPhysChem, 20, 276–284, https://doi.org/10.1002/cphc.201800935, 2019.

Massi, F. and Peng, J. W.: Characterizing Protein Dynamics with NMR R1ρRelaxation Experiments, in: Protein NMR: Methods and Protocols, edited by: Ghose, R., Springer, New York, NY, 205–221, https://doi.org/10.1007/978-1-4939-7386-6_10, 2018.

Nimerovsky, E. and Goldbourt, A.: Insights into the spin dynamics of a large anisotropy spin subjected to long-pulse irradiation under a modified REDOR experiment, J. Magn. Reson., 225, 130–141, https://doi.org/10.1016/j.jmr.2012.09.015, 2012.

Nimerovsky, E., Becker, S., and Andreas, L. B.: Windowed cross polarization at 55 kHz magic-angle spinning, J. Magn. Reson., 349, 107404, https://doi.org/10.1016/j.jmr.2023.107404, 2023.

Nishiyama, Y., Hou, G., Agarwal, V., Su, Y., and Ramamoorthy, A.: Ultrafast Magic Angle Spinning Solid-State NMR Spectroscopy: Advances in Methodology and Applications, Chem. Rev., https://doi.org/10.1021/acs.chemrev.2c00197, 2022.

Oas, T. G., Griffin, R. G., and Levitt, M. H.: Rotary resonance recoupling of dipolar interactions in solid-state nuclear magnetic resonance spectroscopy, J. Chem. Phys., 89, 692–695, https://doi.org/10.1063/1.455191, 1988.

Öster, C., Kosol, S., and Lewandowski, J. R.: Quantifying Microsecond Exchange in Large Protein Complexes with Accelerated Relaxation Dispersion Experiments in the Solid State, Sci. Rep., 9, 11082, https://doi.org/10.1038/s41598-019-47507-8, 2019.

Palmer, A. G. and Massi, F.: Characterization of the Dynamics of Biomacromolecules Using Rotating-Frame Spin Relaxation NMR Spectroscopy, Chem. Rev., 106, 1700–1719, https://doi.org/10.1021/cr0404287, 2006.

Palmer, A. G. I.: NMR Characterization of the Dynamics of Biomacromolecules, Chem. Rev., 104, 3623–3640, https://doi.org/10.1021/cr030413t, 2004.

Palmer, A. G. I.: Enzyme Dynamics from NMR Spectroscopy, Acc. Chem. Res., 48, 457–465, https://doi.org/10.1021/ar500340a, 2015.

Paulson, E. K., Martin, R. W., and Zilm, K. W.: Cross polarization, radio frequency field homogeneity, and circuit balancing in high field solid state NMR probes, J. Magn. Reson., 171, 314–323, https://doi.org/10.1016/j.jmr.2004.09.009, 2004.

Pratihar, S., Sabo, T. M., Ban, D., Fenwick, R. B., Becker, S., Salvatella, X., Griesinger, C., and Lee, D.: Kinetics of the Antibody Recognition Site in the Third IgG-Binding Domain of Protein G, Angew. Chem. Int. Ed., 55, 9567–9570, https://doi.org/10.1002/anie.201603501, 2016.

Quinn, C. M. and McDermott, A. E.: Monitoring conformational dynamics with solid-state R1ρ experiments, J. Biomol. NMR, 45, 5–8, https://doi.org/10.1007/s10858-009-9346-7, 2009.

Rangadurai, A., Szymaski, E. S., Kimsey, I. J., Shi, H., and Al-Hashimi, H. M.: Characterizing micro-to-millisecond chemical exchange in nucleic acids using off-resonance $R1\rho$ relaxation dispersion, Prog. Nucl. Magn. Reson. Spectrosc., 112–113, 55–102, https://doi.org/10.1016/j.pnmrs.2019.05.002, 2019.

Redfield, A. G.: On the Theory of Relaxation Processes, IBM J. Res. Dev., 1, 19–31, https://doi.org/10.1147/rd.11.0019, 1957.

Rovó, P.: Recent advances in solid-state relaxation dispersion techniques, Solid State Nucl. Magn. Reson., 108, 101665, https://doi.org/10.1016/j.ssnmr.2020.101665, 2020.

Rovó, P. and Linser, R.: Microsecond Timescale Protein Dynamics: a Combined Solid-State NMR Approach, ChemPhysChem, 19, 34–39, https://doi.org/10.1002/cphc.201701238, 2018.

Schanda, P. and Ernst, M.: Studying dynamics by magic-angle spinning solid-state NMR spectroscopy: Principles and applications to biomolecules, Prog. Nucl. Magn. Reson. Spectrosc., 96, 1–46, https://doi.org/10.1016/j.pnmrs.2016.02.001, 2016.

Schmidt-Rohr, K., Clauss, J., and Spiess, H. W.: Correlation of structure, mobility, and morphological information in heterogeneous polymer materials by two-dimensional wideline-separation NMR spectroscopy, Macromolecules, 25, 3273–3277, https://doi.org/10.1021/ma00038a037, 1992.

Sekhar, A. and Kay, L. E.: An NMR View of Protein Dynamics in Health and Disease, Annu. Rev. Biophys., 48, 297–319, https://doi.org/10.1146/annurev-biophys-052118-115647, 2019.

Shaka, A. J., Keeler, J., Frenkiel, T., and Freeman, R.: An improved sequence for broadband decoupling: WALTZ-16, J. Magn. Reson. 1969, 52, 335–338, https://doi.org/10.1016/0022-2364(83)90207-X, 1983.

Shcherbakov, A. A., Brousseau, M., Henzler-Wildman, K. A., and Hong, M.: Microsecond Motion of the Bacterial Transporter EmrE in Lipid Bilayers, J. Am. Chem. Soc., 145, 10104–10115, https://doi.org/10.1021/jacs.3c00340, 2023.

Sodickson, A. and Cory, D. G.: Shimming a High-Resolution MAS Probe, J. Magn. Reson., 128, 87–91, https://doi.org/10.1006/jmre.1997.1218, 1997.

Stief, T., Vormann, K., and Lakomek, N.-A.: Sensitivity-enhanced NMR 15N R1 and R1ρ relaxation experiments for the investigation of intrinsically disordered proteins at high magnetic fields, Methods, 223, 1–15, https://doi.org/10.1016/j.ymeth.2024.01.008, 2024.

Stringer, J. A., Bronnimann, C. E., Mullen, C. G., Zhou, D. H., Stellfox, S. A., Li, Y., Williams, E. H., and Rienstra, C. M.: Reduction of RF-induced sample heating with a scroll coil resonator structure for solid-state NMR probes, J. Magn. Reson., 173, 40–48, https://doi.org/10.1016/j.jmr.2004.11.015, 2005.

Tošner, Z., Purea, A., Struppe, J. O., Wegner, S., Engelke, F., Glaser, S. J., and Reif, B.: Radiofrequency fields in MAS solid state NMR probes, J. Magn. Reson., 284, 20–32, https://doi.org/10.1016/j.jmr.2017.09.002, 2017.

Tošner, Z., Sarkar, R., Becker-Baldus, J., Glaubitz, C., Wegner, S., Engelke, F., Glaser, S. J., and Reif, B.: Overcoming Volume Selectivity of Dipolar Recoupling in Biological Solid-State NMR Spectroscopy, Angew. Chem. Int. Ed., 57, 14514–14518, https://doi.org/10.1002/anie.201805002, 2018.

https://doi.org/10.5194/mr-2024-21
Preprint. Discussion started: 19 November 2024

Open Access MAGNETIC RESONANCE Discussions

Vold, R. L., Waugh, J. S., Klein, M. P., and Phelps, D. E.: Measurement of Spin Relaxation in Complex Systems, J. Chem. Phys., 48, 3831–3832, https://doi.org/10.1063/1.1669699, 1968.

Vugmeyster, L., Ostrovsky, D., Greenwood, A., and Fu, R.: Deuteron rotating frame relaxation for the detection of slow motions in rotating solids, J. Magn. Reson., 337, 107171, https://doi.org/10.1016/j.jmr.2022.107171, 2022.

Vugmeyster, L., Rodgers, A., Ostrovsky, D., James McKnight, C., and Fu, R.: Deuteron off-resonance rotating frame relaxation for the characterization of slow motions in rotating and static solid-state proteins, J. Magn. Reson., 352, 107493, https://doi.org/10.1016/j.jmr.2023.107493, 2023.

Xu, K., Pecher, O., Braun, M., and Schmedt auf der Günne, J.: Stable magic angle spinning with Low-Cost 3D-Printed parts, J. Magn. Reson., 333, 107096, https://doi.org/10.1016/j.jmr.2021.107096, 2021.